

Delhi–Hardwar Ridge and surrounding basement structure – Some inferences from deep resistivity sounding measurements

V. Chakravarthi*, S. B. Singh, G. Ashok Babu, B. Veeraiah and Jimmy Stephen

DRS Group, National Geophysical Research Institute, Hyderabad 500 007, India

The hitherto unknown lateral extension of the concealed Delhi–Hardwar Ridge (DHR) towards the east in the Palwal sub-basin of India is inferred from deep resistivity sounding measurements. The resistivity of the ridge is found to be more than 3000 Ohm.m, which is distinct in contrast to the sediment and basement resistivity. The depth of the ridge is estimated to be of the order of 600–800 m below ground level. Analysis of resistivity data across the ridge clearly shows that the basement dips towards the ridge and several depressions within the basement are not uncommon. Further, a significant lateral variation in resistivity of Neogene sediments in and around the DHR indicates post-depositional tectonic activity within the sub-basin. Basement depths estimated compare well with the interpreted depths from aeromagnetic data.

Keywords: Basement structure, deep resistivity sounding, Delhi–Hardwar Ridge, Palwal sub-basin.

THE geoelectrical resistivity method plays a significant role in the exploration of natural resources like groundwater, mineral deposits, hydrocarbons, etc. In regional geophysical surveys, the resistivity method is being used in combination with other geophysical methods such as gravity, magnetics, seismics and magnetotellurics to study the subsurface structures and more particularly, the basement geometry. Dipole resistivity sounding is being used prodigiously in Russia, Canada and other European countries for locating structures such as anticlines, structural and stratigraphic traps, which are favourable for accumulation of hydrocarbons. Owing to the controlled source of energy, the resistivity method attains higher resolution in discriminating layers at shallower depths. Thus the geoelectrical parameters inferred from resistivity measurements pave the way for correcting distorted magnetotelluric (MT) signals at higher frequencies. It can be stated in unequivocal terms that the resistivity method better resolves resistive structures, whereas MT the conductive structures. Therefore, the resistivity and MT methods are complementary to each other in many exploration strategies to infer the subsurface geology.

We have carried out detailed deep resistivity sounding experiments to identify favourable sites for the construction of high-power HVDC earth electrode stations in Palwal sub-basin, Haryana. The study area encompasses long. $77^{\circ}15'06''$ – $77^{\circ}29'04''$ E and lat. $27^{\circ}57'00''$ – $28^{\circ}03'06''$ N, and falls in the Survey of India toposheet 53 H/8 (Figure 1). The investigated area has been identified as Tumasara and Inayatpur blocks (Figure 1). The Tumasara Block is situated about 15 km south of Palwal town on National Highway NH2, and Inayatpur Block is about 18 km southeast of Palwal town. In this article, we present our results to delineate the concealed part of the Delhi–Hardwar Ridge (DHR) and the surrounding basement structure using deep resistivity sounding measurements.

Geology and tectonics

The study area is the northwestern part of the Ganga basin. Figure 2 shows a part of the Ganga basin and adjoining area¹ between long. 74 – 79° E and lat. 24 – 30° N. The sedimentary cover over most part of the Ganga basin is composed of two major stratigraphic and structural sequences representing two main sedimentary stages in the geologic evolution of the basin. The oldest one corres-

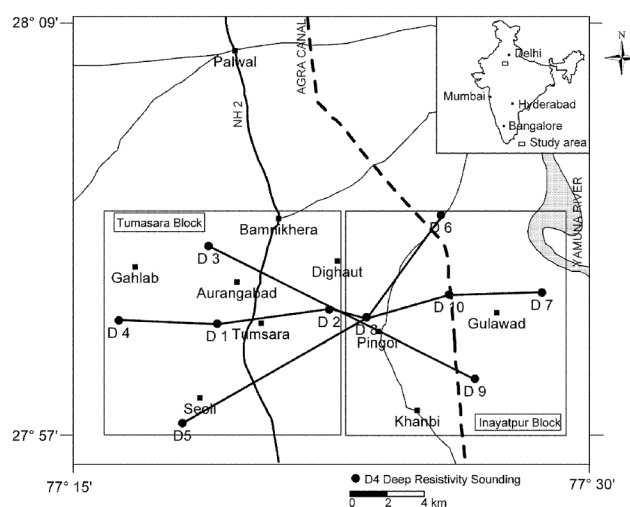


Figure 1. Location map of the Palwal sub-basin, Haryana, India.

*For correspondence. (e-mail: vcvarthi@rediffmail.com)

ponds to the Vindhyan represented by stable-to-unstable shelf sediments composed of quartzarenite–limestone–shale alterations. The youngest sequences unconformably overlying the Vindhyan are the Tertiaries, which composed almost entirely of Siwalik sediments².

The western margin of the basin is delimited by the extension of the Delhi metasediments to the north forming the DHR in the subsurface (Figure 2). The DHR is a north-northeastward extension of the Aravalli Mountain Belt, which stretches from Amba Mata-Deri to Delhi via Ajmer and Jaipur. The DHR comprises quartzite, slate and basic rocks, which belong to the Delhi group³. The Oil and Natural Gas Corporation Limited (ONGC) has reported its northward extension below the Indo-Gangetic Plains at Panipat and Saharanpur. The DHR is about 65–70 km wide between Kalsi (Ponta Sahib) and Chilla (Hardwar). It is estimated to exist at a depth of 2 km at Dehradun³ and becomes gradually deeper towards the north of Mussoorie and Uttarkashi. The Yamuna Tear Fault and Ganga Tear Fault delimit the DHR on the western and eastern sides, where the rivers Yamuna and Ganga flow down from the Lesser Himalayas into the Indo-Gangetic Plains. Neogene sediments overlie the basement in the Palwal sub-basin (northwestern part of the Ganga basin) and the Vindhyan gradually thin out towards the ridge¹, although the Moradabad fault seems to limit the deposition of the Vindhyan sediments to the west (Figure 2).

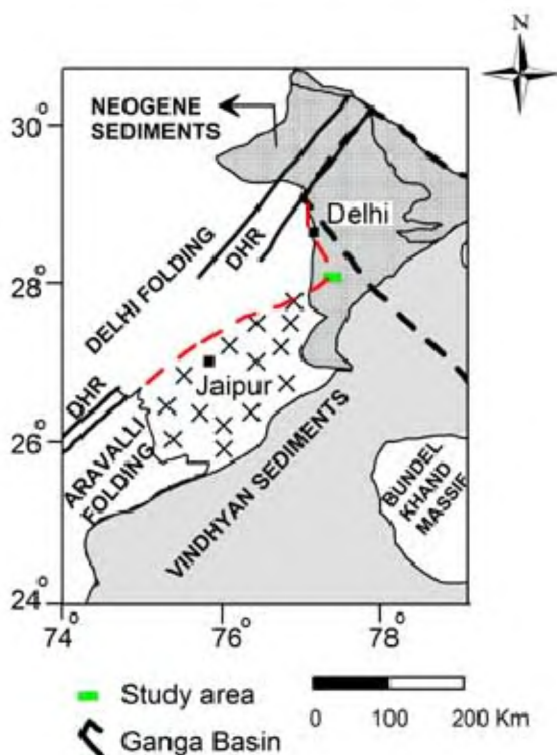


Figure 2. Geology of a part of Ganga basin and adjoining area (modified after Sastri *et al.*¹).

Geophysical surveys and field procedure

We have opted deep resistivity experiments to explore the subsurface geology of the area, because significant resistivity contrast exists between the low-resistive Neogene sediments, DHR and basement structure.

The DC resistivity technique works on the basic principle of studying the nature of resistance offered by subsurface layers or rocks to the flow of electric current sent into the ground. The resistivity, a measure of this resistance, will vary widely from one rock formation to another and several factors such as porosity, fracture geometry and nature of saturating fluids affect the resistivity of rock formations. Therefore, the resistivity method yields subsurface geological information, provided a resolvable resistivity contrast exists between different layers/structures.

In the present survey, the Schlumberger electrode configuration which is least affected by shallow inhomogeneities⁴ is used for making sounding measurements. The schematic representation of a typical sounding layout is shown in Figure 3. The set-up comprises a collinear electrode system where both the current (A and B) and potential electrodes (M and N) are kept in a line. The two current electrodes being the outermost and the potential electrodes being the closest, are kept symmetrical with respect to the centre of the array. During sounding measurements, the current electrode spacing is increased progressively to enable the current to penetrate deeper horizons of the subsurface. Resistivity sounding measurements up to a maximum current electrode separation of 0.5 km were carried out using a portable DC resistivity meter (Terra Science). Eight battery packs, each of which generates 90 V, were connected in series to generate the required voltage. For current electrode separation from 0.5 to 10 km, high-powered deep resistivity equipment (Scintrex) was used. This equipment consists of three major units – generator, transmitter and receiver. The 10 kW generator is capable of producing a three-phase regulated voltage of 210 V at 600 Hz. The transmitter could provide an output voltage up to 3300 V DC and current up to

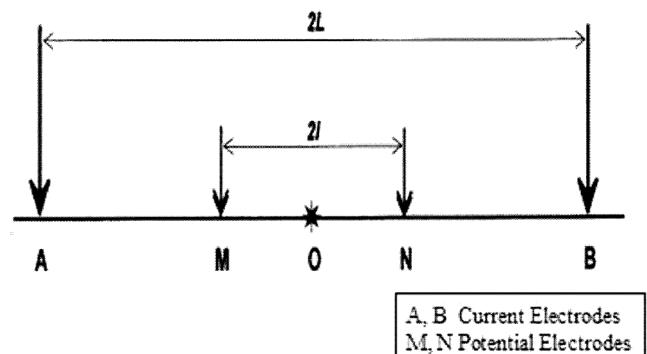


Figure 3. Layout of Schlumberger electrode configuration.

20 A. The total sequence of a transmitting cycle consists of an initial period during which the current is on, followed by three consecutive periods of similar duration during which the current is off, reversed and again switched-off. The duration of each phase can be fixed at 2, 4 or 8 s. In the present study, a duration of 2 s was chosen. The RDC-10 receiver, which has a measuring range from 30 μV to 30 V, was used to record the potential difference across the potential electrodes. Master-slave communication sets were used for maintaining communication between field personnel and the operator along the survey line.

Each time the current is sent, the potential difference (δV) between two non-polarizable electrodes on the surface is being measured along with input current (I), from which the apparent resistivity is computed based on the equation

$$\rho_a = K(\delta V/I),$$

where K is the geometrical factor given by Keller and Frischnecht⁵ as:

$$K = \frac{\pi(L^2 - l^2)}{2l}.$$

The plot of the measured apparent resistivity (ρ_a) against the half current electrode separation ($AB/2$) on a double log graph paper having a modulus of 62.5 mm, forms the resistivity sounding curve.

In the present study, a total of ten deep resistivity soundings with a maximum current electrode separation of 10 km were conducted, five each in the Tumasara and Inayatpur blocks respectively. The locations of sounding stations are shown in Figure 1.

Interpretation

Interpretation of resistivity sounding data is implicitly a mathematical exercise of approximating the subsurface by a series of horizontal layers, and identifies the parameters (thickness and true resistivities) such that the theoretical apparent resistivities mimic the observed ones. Interpretation of resistivity data is generally carried out as a two-pronged strategy; one is qualitative and the other quantitative. In qualitative interpretation, the nature and characteristics such as gradient, sharpness and width of each sounding curve are studied. Preparation of pseudo resistivity cross-sections can further help in deciphering the resistivity distribution of the subsurface. These pseudo-sections are prepared by making contours of the observed apparent resistivities by plotting them at each current electrode separation ($AB/2$) on the y-axis, with the corresponding sounding station on the x-axis of a graph paper. In quantitative interpretation, the subsurface is approximated to a series of layers and the true parameters (resis-

tivity and thickness) are estimated by adopting various forms of optimization techniques. The number of layers to be incorporated in modelling and inversion can be identified from the characteristics of the respective sounding curve. The effect of lateral inhomogeneities is removed in each sounding curve⁴, so as to attribute the observed signal entirely to vertical distribution of resistivity. Although data interpretation by curve-matching^{6,7} is in vogue, computer algorithms based on optimization techniques become much popular owing to their efficiency and speed in computation.

Quantitative interpretation of sounding data consists of two steps: (i) forward modelling and (ii) inversion. In forward modelling, the apparent resistivity response of a given model is computed⁸⁻¹³ and in inversion¹⁴⁻²¹ the true parameters of the geoelectrical model are estimated automatically by fitting the theoretical response of the model to the observed one in an iterative approach, until the difference between these two responses becomes negligible.

Figures 4 and 5 show the observed sounding curves in Tumasara and Inayatpur blocks. The sounding curves at stations D3–D5 in the Tumasara Block have distinct characteristics in comparison to the ones observed at D1 and D2 (Figure 4). The ascending nature of sounding curves beyond a current electrode separation of 2 km at D3–D5 (Figure 4) indicates a resistive substratum comparatively at a shallower depth. The descending nature of sounding curves D1 and D2 at larger current electrode separation (Figure 4) suggests that the thickness of Neogene sediments is of some significance. In the Inayatpur Block, the influence of resistive basement is clearly seen

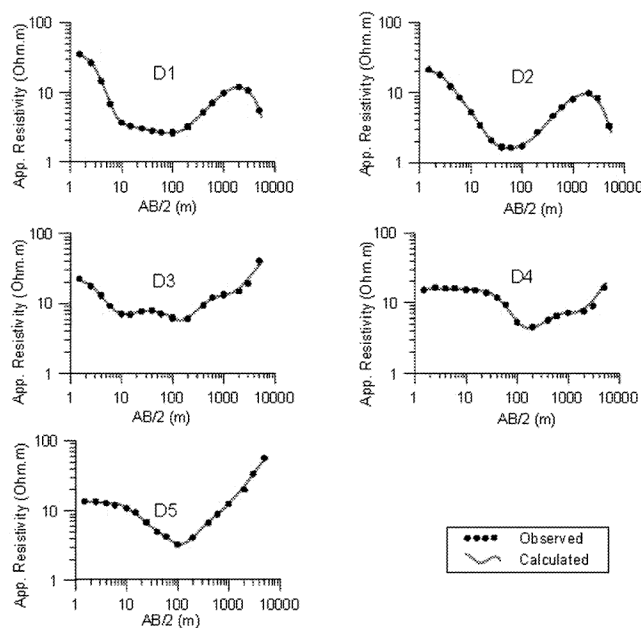
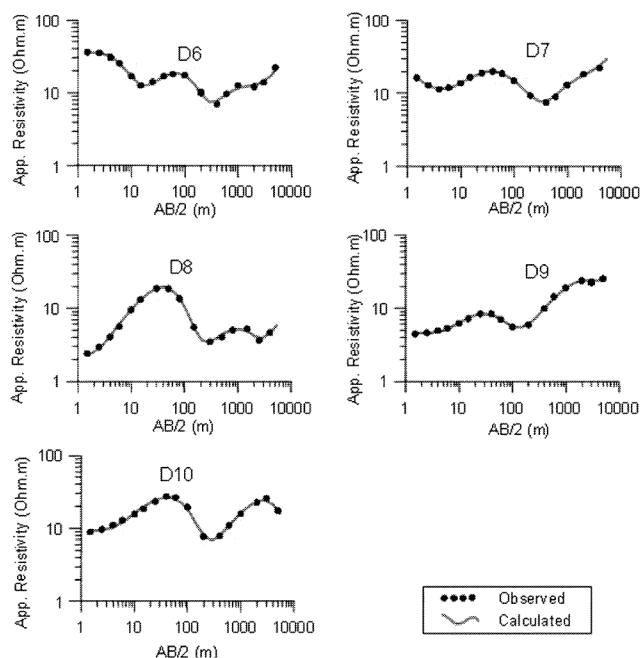


Figure 4. Measured and theoretical resistivity sounding curves, Tumasara Block, Palwal sub-basin, India.

Table 1. Interpreted geoelectrical parameters of deep resistivity sounding data in Palwal sub-basin, Haryana, India

Sounding no.	True resistivity (Ohm.m)							Thickness (m)							Total depth (m)
	ρ_1	ρ_2	ρ_3	ρ_4	ρ_5	ρ_6	ρ_7	h_1	h_2	h_3	h_4	h_5	h_6	h_7	
Tumasara Block															
D1	39.3	3.22	2.43	27.9	0.0149			1.63	14.3	148	1008				1172
D2	22.9	6.35	1.49	22.6	0.0116			1.65	5.42	105	894				1006
D3	23	6.06	9.41	3.39	67.9	3.52	4638	1.67	8.27	28.9	88.7	113	382		622
D4	15.6	3.6	14.3	1.48	3843			27.3	162	304	318				812
D5	13.2	5.08	0.781	14.8	3193			7.27	34.5	23.5	785				851
Inayatpur Block															
D6	36.1	5.89	26.5	1.66	73	4.25	420	3.81	5.68	56.3	68.3	145	781		1061
D7	21.6	9.65	24.9	10.5	3.07	91.9	482	0.761	4.03	122.4	137	261	602		1127
D8	2.0	140	2.32	9.8	0.769	660		1.88	5.99	160	486	625			1279
D9	4.47	12.4	4.2	234	4.4	430		4.65	15.8	143	161	830			1154
D10	9.33	36.7	4.53	82.2	0.07			4.03	37	210	937				1188

**Figure 5.** Measured and theoretical resistivity sounding curves, Inayatpur Block, Palwal sub-basin, India.

in the sounding curves at D6–D9; however, at D10 it is not repeated (Figure 5).

For qualitative interpretation, pseudo-apparent resistivity cross-sections along three selected traverses connecting D4–D1–D2–D8–D10–D7, D5–D8–D6 and D3–D2–D9 are prepared and shown in Figure 6 *a–c* respectively. It can be seen from Figure 6 *a* that a thick low-resistivity zone with 3–5 Ohm.m corresponds to the Neogene sequence existing between D1 and D2. A similar low-resistivity zone can also be seen at D8 along the traverse D5–D8–D6 (Figure 6 *b*) and also on either side of D2 along the traverse D3–D2–D9 (Figure 6 *c*). A significant lateral variation in resistivity observed at D8 (Figure 6 *a* and *b*)

is due to the Pingor fault. A low-resistivity zone of about 4 Ohm.m extends to larger depths along the fault structure (Figure 6 *a* and *b*). A moderate resistive layer of more than 22 Ohm.m sandwiched between a pair of low-resistivity zones can be seen to the east of D8 (Figure 6 *b*).

Each sounding curve is inverted in terms of geoelectrical parameters¹⁵, and subsequently translated to subsurface geology. The resistivity of Neogene sediments are ascertained by test soundings near by deep boreholes that exist to the west of Dighaut (Figure 1) and used to constrain the interpretation of other sounding data. The calculated resistivities of ten soundings subsequent to inversion are shown in Figures 4 and 5 along with the observed ones. The interpreted geoelectrical parameters of each sounding are given in Table 1. Geoelectrical cross-sections along the three selected traverses are shown in Figure 7. It is evident from Figure 7 *a–c* that a high-resistivity zone with more than 3000 Ohm.m is seen at stations D3–D5 at a depth of about 500–800 m below ground level. This high-resistivity zone is the subsurface manifestation of the DHR. We are of the opinion that the lateral extent of the concealed DHR towards the east in Palwal sub-basin is more than that shown by Sastri *et al.*¹. The inferred eastward extension of the DHR from the present study is shown as dotted line in red in Figure 2. An elongated, oval-shaped gravity high²² trending north-south in the southern and southwestern part of Delhi, further substantiates the eastward extension of the DHR (Figure 8). In addition, the short-wavelength anomaly indicates that the ridge might have been emplaced at a moderate depth. To the north of Delhi the gravity signature is not so conspicuous perhaps due to (i) insignificant density contrast between the DHR and surrounding formation or (ii) the deficiency of mass below the DHR or a combination of (i) and (ii).

A low-resistivity zone of 10–100 Ohm.m corresponding to a thick pile of Neogene sediments is seen in all the traverses with varying thickness (Figure 7 *a–c*). It can be

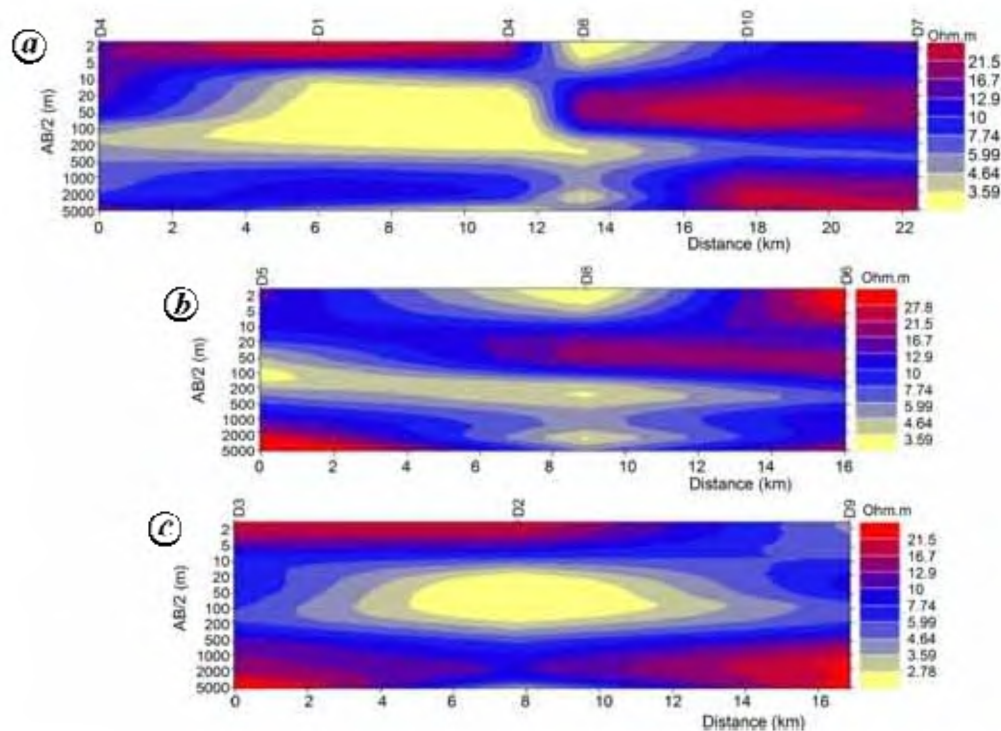


Figure 6. Pseudo apparent resistivity cross-sections along traverses (a) D4–D1–D2–D8–D10–D7, (b) D5–D8–D6 and (c) D3–D2–D9.

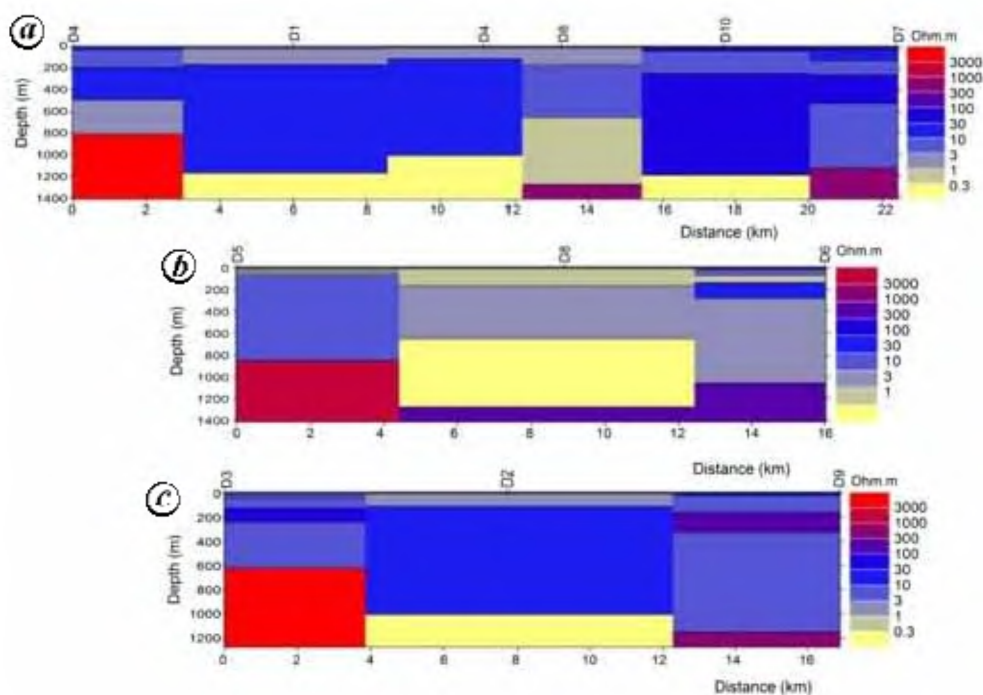


Figure 7. Geoelectrical cross-sections along traverses (a) D4–D1–D2–D8–D10–D7, (b) D5–D8–D6 and (c) D3–D2–D9.

noted from Figure 7 *a* that even in the Neogene sequence a significant lateral variation in resistivity is observed, across the Pingor fault. This fault structure separates the low-resistivity Neogene sediments on the west (13 to

30 Ohm.m) from relatively high-resistivity sediments to the east (30–100 Ohm.m). The high-resistivity of sediments indicates that they are relatively compacted than the corresponding one in the vicinity of the DHR. Similar fea-

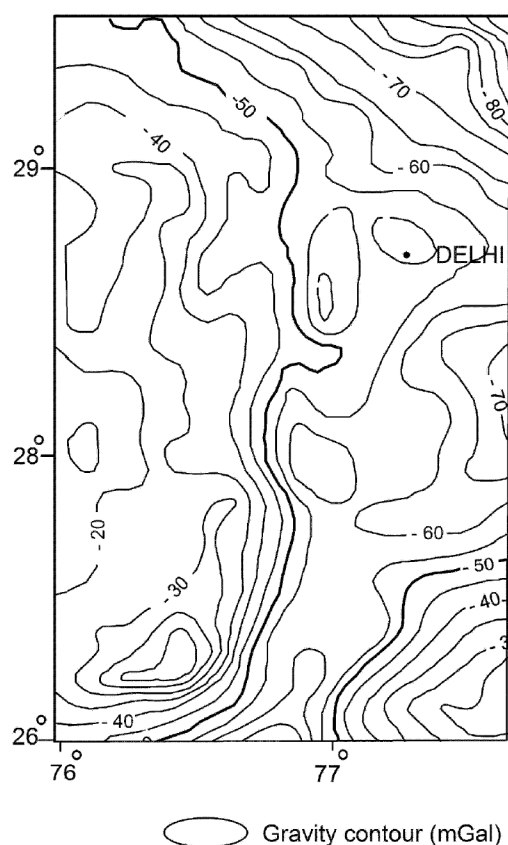


Figure 8. Bouguer gravity anomaly of the western part of the Ganga basin, India (modified after Mishra and Laxman²²).

tures can be seen in other traverses too (Figure 7 b and c). Saraf and Das²³ have shown that the Siwalik sediments have undergone severe folding in the frontal region of Himalayan foothills and such an activity could not be ruled out in erstwhile parts of the Ganga basin.

The depth of the basement estimated from the present inversion is about 1.2 km near D7–D9 (Figure 7 a and c). Based on the interpretation of aeromagnetic data, Agocs²⁴ inferred that the thickness of the Neogene sediments could be 1 km in this region. At locations D1, D2, D6 and D10 (Figure 7 a–c), the depth to the basement (>1.4 km) could not be estimated accurately as the sounding curves show a decreasing trend at larger current electrode separation. Variation in the estimated depths in all traverses reveals that the basement is non-uniform in nature and several depressions within the basement are not uncommon. Sharma *et al.*²⁵ also reported several local scale basement depressions in the Ganga basin. Further, the resistivity of the basement (300–600 Ohm.m) estimated from the interpretation of sounding data differs substantially from that of the DHR and Neogene sediments. The abnormal high resistivity (>3000 Ohm.m) found at stations D3–D5 would correspond to the DHR. In addition, it can be seen from Figure 7 a–c that by and large the basement deepens from east to west towards the DHR.

Conclusions

It is reported here for first the time based on the interpretation of deep resistivity sounding data that the DHR extends further east in the Palwal sub-basin, Haryana, than inferred from earlier studies. Resistivity of the DHR is found to be more than 3000 Ohm.m, whereas resistivity of Neogene sediments and basement are in the range of 0.1–100 and 300–600 Ohm.m respectively. A significant variation in resistivity of Neogene sediments is found across the Pingor fault. The sediments on the eastern side of the Pingor fault show higher resistivity probably suggesting that they are relatively compacted. The estimated thickness of Neogene sediments from the interpretation of deep resistivity sounding data compares well with those inferred from aeromagnetic data.

1. Sastri, V. V., Bhandari, L. L., Raju, A. T. R. and Datta, A. K., Tectonic framework and subsurface stratigraphy of the Ganga basin. *J. Geol. Soc. India*, 1971, **12**, 222–233.
2. Uniyal, A. K., Chandra, U., Nain, K., Dhawan, R., Banerji, V. and Chandra, K., Environmental studies in Ganga basin through stable isotope ratios. In *Proceedings of the Second Seminar on Petroli-ferous Basins of India* (ed. Biswas, S. K.), Indian Petroleum Pub-lishers, Dehra Dun, 1994, vol. 3, pp. 173–184.
3. Pal, D., Srivastava, R. A. K. and Mathur, N. S., Influence of Delhi–Hardwar–Harsil Ridge (DHHR) on basin configuration in Himalayan foothills belt during Tertiary. *Himalayan Geol.*, 2000, **21**, 133–144.
4. Bhattacharya, P. K. and Patra, H. P., *Direct Current Geoelectric Sounding: Principles and Interpretation*, Elsevier, UK, 1968, pp. 99–101.
5. Keller, G. V. and Frischnecht, F. C., *Electrical Methods in Geo-physical Prospecting*, Pergamon, New York, 1967, p. 519.
6. Kalenov, E. N., Interpretatsia Krivikh Vertikalnogo Elektriche-kogo Zondirovaniya, Gostoptekhizdat, Moskva, 1957, p. 470.
7. Compagnie Generale De Geophysique, *Master Curves for Electri-cal Sounding*, European Association for Exploration in Geophys-ics, The Hague, 1963, 2nd edn, p. 49.
8. Mooney, H. M., Orellana, E., Pickett, H. and Tornheim, L., A esistivity computation method for layered earth models. *Geophys-ics*, 1966, **31**, 192–203.
9. Koefoed, O., *Geosounding Principles, 1 – Resistivity Sounding Measurements*, Elsevier, The Netherlands, 1979, p. 276.
10. Ghosh, D. P., The application of linear filter theory to the direct interpretation of geoelectrical resistivity sounding measurements. *Geophys. Prospect.*, 1971, **19**, 192–217.
11. Das, U. C. and Gosh, D. P., The determination of filter coefficient for the computation of standard curves for dipole resistivity sounding over layered earth by linear digital filtering. *Geophys. Prospect.*, 1974, **22**, 765–780.
12. O'Neill, D. J., Improved linear filter coefficients for application in apparent resistivity computations. *Bull. Aust. Assoc. Explor. Geo-phys.*, 1975, **6**, 104–109.
13. Guptasarma, D., Optimization of short digital linear filters for increased accuracy. *Geophys. Prospect.*, 1982, **30**, 501–514.
14. Jupp, D. L. B. and Vozoff, K., Stable iterative methods for the inversion of geophysical data. *Geophys. J. R. Astron. Soc.*, 1975, **42**, 957–976.
15. Murakami, Y., Zerilli, A. and Bisdorf, R. J., A computer program for the automatic inversion of Schlumberger soundings using multi-layer interpretation followed by Dar Zarrouk reduction. Open File Report, US Geological Survey, 1986.

RESEARCH ARTICLES

16. Pous, J., Marcuello, A. and Queral, P., Resistivity inversion with a priori information. *Geophys. Prospect.*, 1987, **35**, 590–603.
17. Bhattacharya, B. B. and Roy, I. G., A method of inversion and its application to VES measurements. In *Advances in Geophysics* (ed. Bhattacharya, B. B.), Oxford and IBH Publishing Co, 1988, pp. 42–64.
18. Roy, K. K. and Rathi, O. P., Resistivity inversion using resistivity signal partitions. *Gerlands Beitr. Geophys.*, 1988, **97**, 472–494.
19. Muirhead, E. A. and Pederson, L. B., 1D inversion of DC resistivity data using a quality-based truncated SVD. *Geophys. Prospect.*, 2001, **49**, 387–394.
20. Andersen, K. E., Brooks, S. P. and Hansen, M. B., Bayesian inversion of geoelectrical resistivity data. *J. R. Stat. Soc.*, 2003, **65**, 619–642.
21. Auken, E. and Christiansen, A. V., Layered and laterally constrained 2D inversion of resistivity data. *Geophysics*, 2004, **69**, 752–761.
22. Mishra, D. C. and Laxman, G., Some major tectonic elements of western Ganga basin based on analysis of Bouguer anomaly map. *Curr. Sci.*, 1997, **73**, 436–440.
23. Saraf, A. K. and Das, J. D., Neogene deformation of Siwaliks affected by the Delhi–Hardwar ridge as seen in satellite data, India. *Curr. Sci.*, 1997, **73**, 877–880.
24. Agocs, W. B., Airborne magnetometer survey. 1. Indo-Gangetic Plains. 2. Rajasthan. Report submitted to Government of India, 1957.
25. Sharma, R., Hansi, J. S. and Mudiar, B., Stratigraphy, tectonics and hydrocarbon prospects of the Matheran Formation in Bahraich depression, Ganga basin. *Himalayan Geol.*, 2000, **21**, 177–188.

ACKNOWLEDGEMENTS. We thank the anonymous reviewers and the reviewing editor for useful suggestions to improve the manuscript. Dr V. P. Dimri, Director, National Geophysical Research Institute, Hyderabad is acknowledged for constant encouragement and permission to publish this paper. We also thank Mr E. Janna Reddy for his help during field data collection. The results presented here are the outcome of a project sponsored by the POWERGRID Corporation of India Ltd, New Delhi.

Received 16 June 2006; revised accepted 25 March 2007
